World Journal of Chemistry 9 (2): 33-40, 2014
ISSN 1817-3128

DOI: 10.5829/idosi.wjc.2014.9.2.1111

Photoluminescent Properties of Eu^{3+}, Ce^{3+}, Tb^{3+} Doped $LaPO_4$ Phosphors

[1]Niyaz Parvin Shaik, [2]N.V. Poornachandra Rao and [3]K.V.R. Murthy

[1]Department of Physics, Government Junior College,
Sathupally, Khammam District, A.P-507303, India
[2]Department of Physics, Rajiv Gandhi University Knowledge Technologies,
IIIT, Basara-504101, AP, India
[3]Display Materials Laboratory, Applied Physics Department,
Faculty of Technology and Engineering, M.S University of Baroda, Baroda-390001, India

Abstract: Pure $LaPO_4$ and $LaPO_4$:Eu (0.5mol%), Ce(0.5 mol%), Tb (0.5mole%) phosphors were synthesized by the solid-state reaction method. X-ray diffraction (XRD), scanning electron microscopy (SEM), Fourier transform infrared spectroscopy (FT-IR), photoluminescence (PL) spectra and the particle size analysis were used to characterize these samples. The XRD results reveal that the synthesized $LaPO_4$:Eu(0.5 mol%), Ce(0.5 mol%), Tb (0.5mole%) phosphors are well crystalline and assigned to the monoclinic structure with a main (120) diffraction peak. The calculated crystallite size of pure $LaPO_4$ and $LaPO_4$:Eu, Ce, Te phosphors were 67.6nm and 64.1nm respectively. Upon excitation at 254nm wavelength, the emission spectrum of pure $LaPO_4$ phosphor emits a maximum intensity peak at 469(blue)nm. In the emission spectrum of LaPO4:Eu^{3+}, Ce^{3+}, Tb^{3+}phosphor, the low contributions of the red(614nm) $^5D_0$-$^7F_2$ emissions and the high intensity of the orange (594nm)$^5D_0$-$^7F_1$ emission results in high color purities. The most intense emissions appearing in the 580-622nm region is responsible for the strong orange luminescence observed in the Eu, Ce Tb doped $LaPO_4$ phosphor whose CIE colour coordinates are x = 0.57 and y = 0.43.Thus the prepared phosphors can be used as an orange emitting material in the field of illuminations and display devices.

Key words: Photoluminescence · XRD · SEM · FTIR · Phosphor · Rare-ea4rth ions · Solid state reaction technique · CIE · Particle size analysis

INTRODUCTION

Inorganic luminescent materials are nowadays widely employed in many quotidian devices and, for this, studies on their obtainment, spectroscopic behaviour and applications have been remarkable. The luminescence of trivalent lanthanide ions has found applications in lighting, lasers, optical telecommunications, medical diagnostics and various other fields.Lanthanide compounds have been extensively used as optoelectronic devices and biological fluorescence labeling because of their special optical, electronic and chemical properties resulting from the 4f electron configurations [1-5]. In recent years, lanthanide orthophosphates ($LnPO_4$) have attracted much interest for the potential applications as phosphors, proton conductors, sensors, catalysts, ceramic materials and heat-resistant materials [6] based on their interesting properties, such as low water solubility [7], high thermal stability [8], high index of refraction and high concentrations of lasing ions[9] and soon. Furthermore, lanthanide phosphates have been shown to beause useful host lattice for doping lanthanide ions to prepare phosphors emitting a wide range of colors [10-13]. The luminescent properties of rare-earth phosphates can be conferred by the presence of lanthanide (III) ions as activators due to their intense and narrow emission bands arising from f_f transitions, which are proper for the generation of individual colours in multiphosphor devices [14-16]. So, the red $^5D_0$?$^7F_2$ (610nm), green $^5D_4$-$^7F_5$ (545 nm) and blue $^1D_2$-$^3F_4$ (450 nm) emissions of Eu^{3+}, Tb^{3+} and

Corresponding Author: Niyaz Parvin Shaik, Department of Physics, Government Junior College, Sathupally, Khammam District, A.P-507303, India.

Tm^{3+}, respectively, can be used for the design of novel phosphors [17]. $LaPO_4$ is a well-known host used to elaborate the luminescent materials for lighting phosphors [18], optical amplifiers and lasers [19] as well as for the other applications. It is known that the $LaPO_4$ has a monoclinic phase of monazite structure crystallographically, wherein La^{3+} ion is nine coordinated to oxygen atoms, four oxygens forming a distorted tetrahedron interpenetrating a quasiplanar pentagon formed by other five [20]. The La^{3+} ion site in the monazite structure can be easily substituted by any other lanthanide ions. The partial substitution of Eu^{3+} or Tb^{3+} to La^{3+} gives rise to efficient luminescent phosphors. Several researchers have reported the syntheses of $LaPO_4$ particles via various methods such as solid-state reaction [21, 22], spray pyrolysis [23] or hydrothermal methods [24, 25].

In this paper $LaPO_4$ and $LaPO_4$:Eu^{3+} (0.5mol%) Ce^{3+} (0.5mol%) Tb^{3+} (0.5mol%) phosphors prepared by the solid state reaction method in air at 1200°C and their luminescent properties were studied. Optimization of the concentration of activator ions incorporated into the host lattice during the synthesis of the phosphor powders is essential for developing highly luminescent RE^{3+} doped nanocrystalline phosphors as well as for the growth of grain particles. Photoluminescence studies and CIE co-ordinates of $LaPO_4$: Eu^{3+} (0.5mol%)Ce^{3+}(0.5 mol%) Tb^{3+} (0.5mol%) phosphors reveals that the emission colour varies from blue to orange. So this material may be a potential luminescent material.

Experimental

Synthesis: Pure $LaPO_4$ and $LaPO_4$: Eu(0.5mole%), Ce(0.5mole%), Tb (0.5mole%) phosphor powders were synthesized by using the conventional solid-state reaction method. The formation of the phosphor powders occurs according to the following chemical equation.

$$La_2O_3 + 2NH_4H_2PO_4 \rightarrow 2LaPO_4 + 2NH_4OH + H_2O$$

$$La_2O_3 + 2NH_4H_2PO_4 + 2Eu_2O_3 + 2CeO_2 + 1/2Tb_4O_7 \rightarrow 2LaPO_4: Eu^{3+}, Tb^{3+}, Ce^{3+}$$

The starting materials were lanthanum oxide (La_2O_3), Diammonium Hydrogen Phosphate [$(NH_4)_2 H_2 PO_4$) and Europium Oxide (Eu_2O_3) Ceric Oxide (CeO_2), Terbium oxide (Tb_4O_7) of 99.9% purity. They were weighed with a certain stoichiometric ratio. The composite powders were grinded in an agate mortar and then placed in an alumina crucible with the lid closed. After the powders had been sintered at 1200°C for 3 hr in a muffle furnace and then cooled to room temperature. All the samples were again ground into fine powder using an agate mortar and pestle about an hour.

Characterization: The crystalline structure of the products was investigated by using an X-ray diffractometer (PANalytical's X-ray diffractometers X'Pert PRO) with Cu Ká radiation. The morphology of the nanoparticles was observed by using a scanning electron microscope (TESCAN VEGA3 SEM) with a tungsten heated filament. The emission and the excitation spectra of the synthesized powders were characterized with a spectroflurophotometer (Shimadzu RF–5301 PC) with xenon lamp as excitation source. Infrared spectra for the prepared solid nano powders were recorded in the range between 400 and 4000 cm^{-1} on a Fourier-transform spectrometer (Bruker Vector 22 FT-IR Spectrometer). The particle size was measured by using laser based system Malvern Instrument, U.K. The Commission International de l'Eclairage (CIE) co-ordinates were calculated by the spectrophotometric method using the spectral energy distribution. The chromatic coordinates (x, y) of prepared materials were calculated with colour calculator version 2, software from Radiant Imaging [26].

RESULTS AND DISCUSSIONS

Crystal Structure of $LaPO_4$ and $LaPO_4$:Eu^{3+}, Ce^{3+}, Tb^{3+} Phosphors: Fig. 1 shows the X-ray diffraction (XRD) patterns of synthesized samples of $LaPO_4$ and $LaPO_4$:Eu^{3+} (0.5mol%) Ce^{3+}(0.5 mol%) Tb^{3+} (0.5mol%) phosphor powders. The XRD spectra consist of three strong peaks and several weak peaks: The three main peaks occur at 2θ=26.81, 28.65 and 31°. These peaks correspond to the diffractions from the (200), (120) and (012) planes of $LaPO_4$ respectively. The relatively weak multipeaks centered at 21.21, 34.39, 41.99 and 48.23° are attributed to the diffraction from the (111), (202), (311) and (132) planes, respectively. The intensity of peaks reflected the high degree of crystallinity of the nanoparticles. However, the diffraction peaks are broad which indicating that the crystalline size is very small. All the diffraction peaks could be well indexed to JCPDS: 84-0600, which indicated a monoclinic structure LaPO4 (space group $P2_1/n$) with a main diffraction peak (120). No spurious diffractions due to crystallographic impurities are found.

Table 1: Unit cell lattice constants of the sample powders

Samples	a (nm)	b (nm)	c (nm)	β angle (deg)	Cell volume (nm^3)
JCPDS-84-0600	0.6825	0.7057	0.64822	103.21	0.3039
$LaPO_4$ phosphor	0.6827	0.70477	0.63968	103.21	0.3077
$LaPO_4$:Eu^{3+} phosphor	0.6837	0.7074	0.6425	103.66	0.3007
$LaPO_4$:Eu^{3+}, Ce^{3+} phosphor	0.6779	0.7032	0.6370	103.45	0.3037
$LaPO_4$:Eu^{3+},Ce^{3+}, Tb^{3+} phosphor	0.6831	0.7075	0.6412	103.46	0.3099

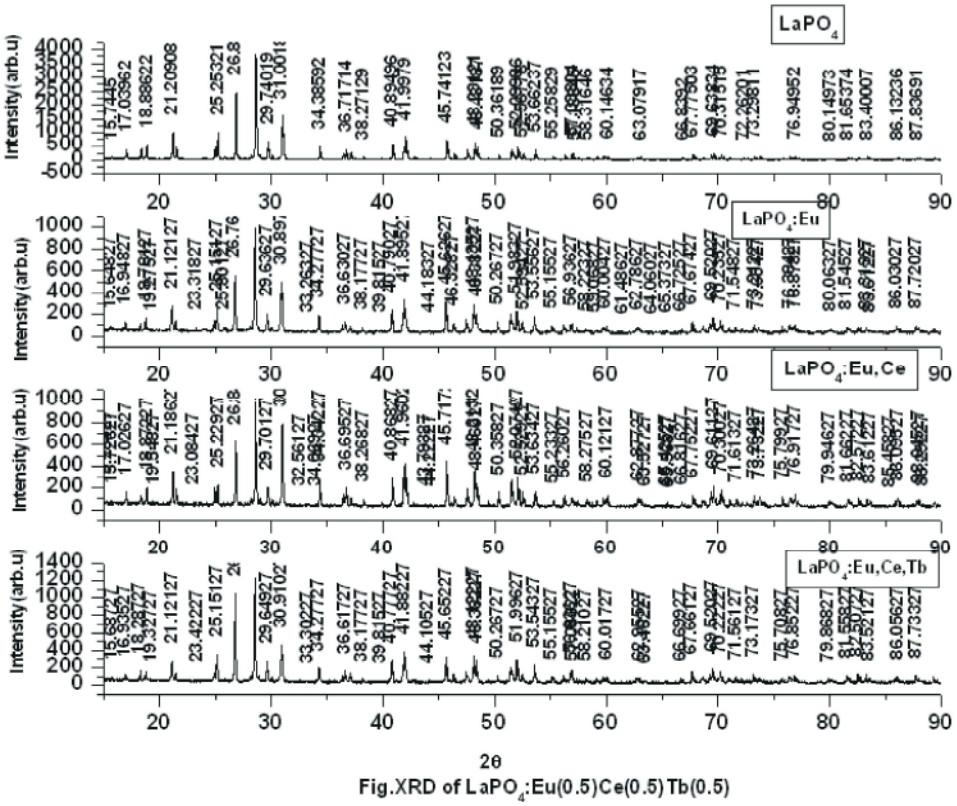

Fig. 1: XRD of pure $LaPO_4$, $LaPO_4$:Eu(0.5mol%) Ce^{3+}(0.5 mol%) and $LaPO_4$: Eu(0.5mole%), Ce(0.5mole%), Tb (0.5mole%)

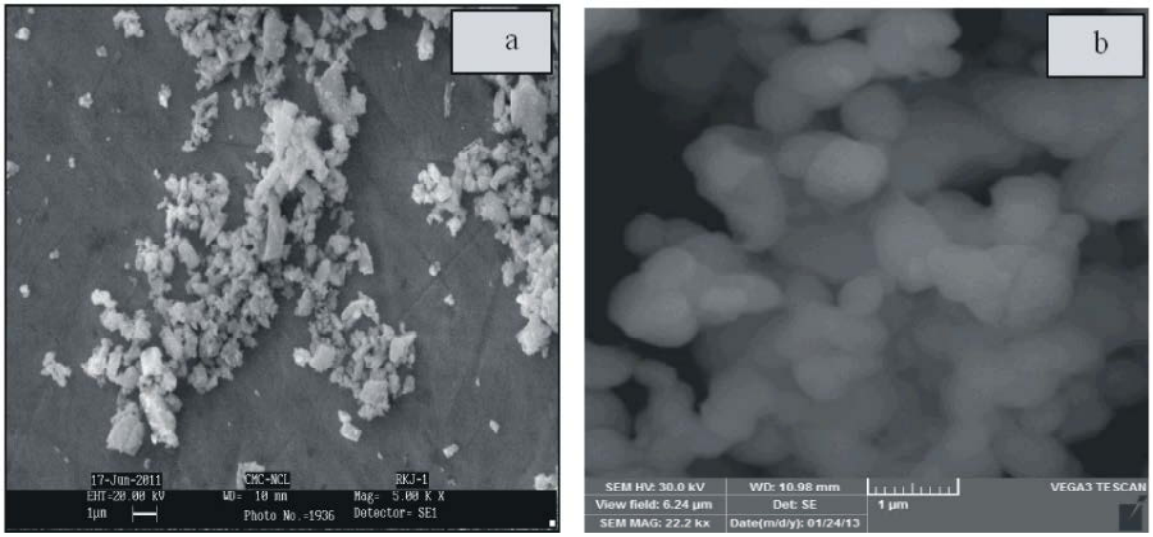

Fig. 2: SEM images of pure $LaPO_4$ and $LaPO_4$:Eu^{3+} $Ce^{3+}$$Tb^{3+}$phosphor

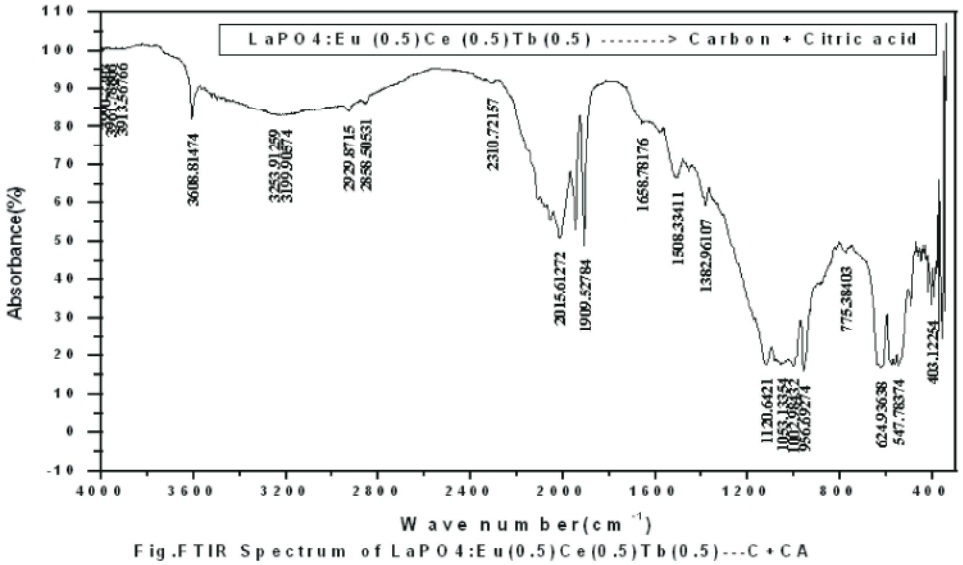

Fig. 3: FTIR spectrum of $LaPO_4$:Eu, Ce, Tb

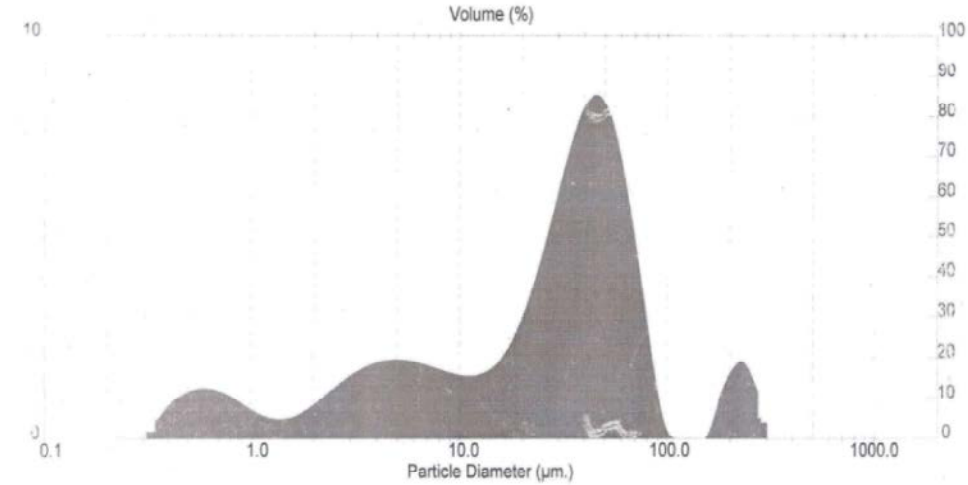

Fig. 4: Particle size distribution histogram of $LaPO_4$:Eu, Ce, Tb phosphors

The average particle size has been estimated by using the Debye-Scherrer formula $D= 0.9\ \lambda / \beta \cos\theta$, where λ is the wave length of the X-ray ($\lambda = 1.54A°$), β is FWHM (full width at half maximum), θ is the diffraction angle and D is the particle diameter size. The average size of a particle of $LaPO_4$ phosphor and $LaPO_4:Eu^{3+,}$ Ce^{3+}, Tb^{3+} (0.5mol%) phosphor are 67.6nm and 64.1nm respectively. This confirms the formation of nano crystalline size phosphor, via solid state reaction method.Unit cell parameters of the sample powders was shown in Table 1.

Morphology of $LaPO_4$ and $LaPO_4:Eu^{3+}$, Ce^{3+}, Tb^{3+} Phosphors: Fig. 2(a, b) are typical SEM images of the morphology of the synthesized nanoparticles of pure $LaPO_4$ and $LaPO_4:Eu^{3+,}$ Ce^{3+} Tb^{3+} phosphors. SEM images attest for the obtainment of homogeneous solids, which occur as micrometric aggregates of nanosized structures. The particles composing these micro aggregates have a spherical shape and sizes ranging from 0.2-1µm. The grain sizes of the samples estimated from the SEM picture is larger than that obtained from XRD analysis. The observation of some larger nanoparticles may be attributed to the fact that the nanoparticles have the tendency to agglomerate due to their high surface energy.

FTIR Analysis of $LaPO_4$ and $LaPO_4:Eu^{3+}$, Ce^{3+}, Tb^{3+} Phosphors: FTIR analysis was carried out to determine the chemical bonds in a molecule. Fig. 3 shows the FTIR

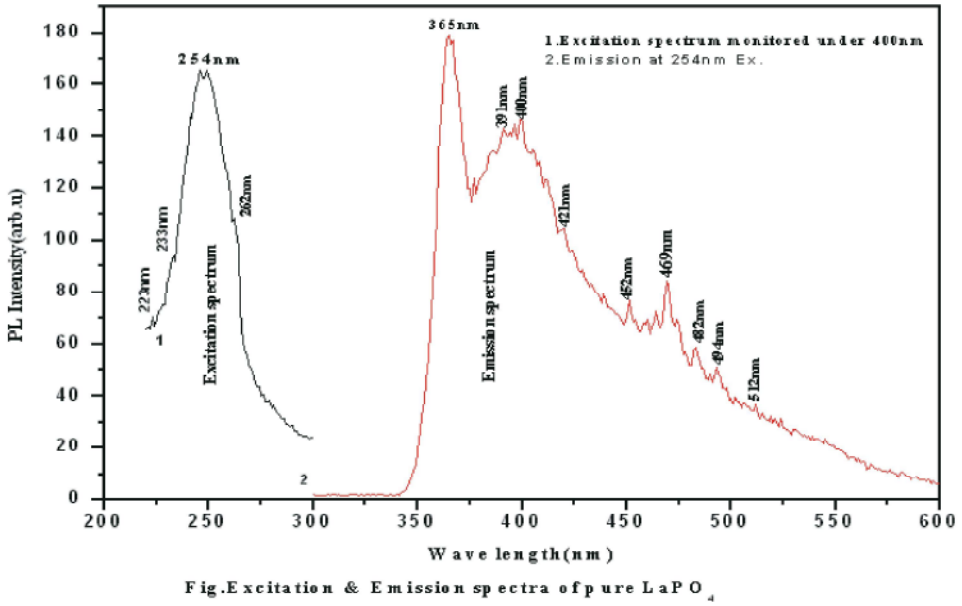

Fig. 5(a): Excitation and Emission spectrum of pure $LaPO_4$

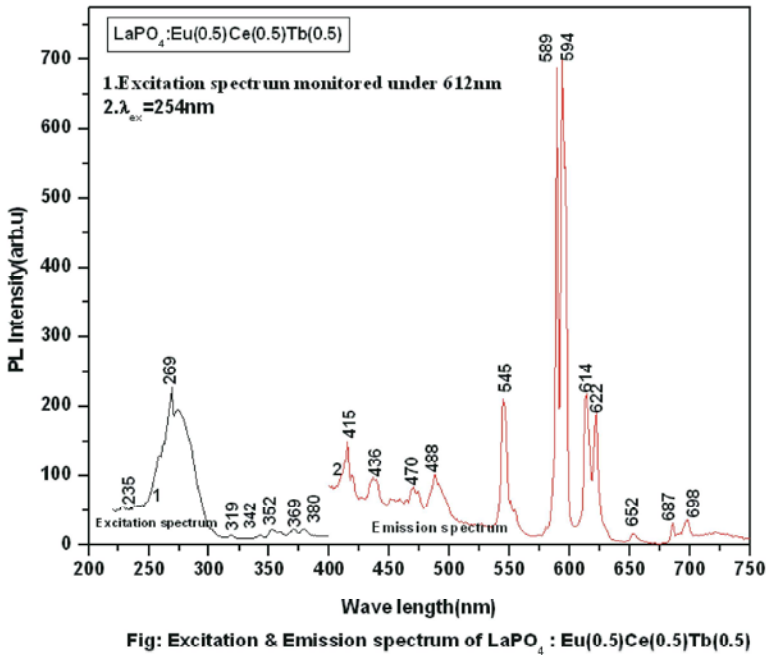

Fig. 5(b): Excitation and emission spectrum of $LaPO_4$:Eu, Ce, Tb phosphor

spectrum of LaPO4:Eu(0.5)Ce(0.5)Tb(0.5). The absorption bands at 3608 and 1658cm^{-1} can be assigned to physical adsorbed OH and H_2O for all the samples. The characteristic vibrations of phosphate (PO_4^{3-}) are obvious. The two bands located at 624 and 547 cm^{-1} are clearly observed in the ν_4 region of the vibrations of PO^{3-}_4 groups. The bands at1053cm^{-1} can be attributed to the ν_3 anti-symmetric stretching of P–O band. The shoulder at 956cm^{-1} can be assigned to the ν_1 vibration of PO_4^{3-} groups [27]. The ν_2 vibration at low wave number is not observed in the studied range of wave numbers. Furthermore, C–H stretching vibration at 1382cm^{-1} can be detected.

Particle Size Analysis: The Particle size distribution histograms of $LaPO_4$:Eu(0.5) Ce(0.5) Tb(0.5) phosphor particles synthesized using the solid state reaction method are illustrated in Fig. 4. The prepared phosphor

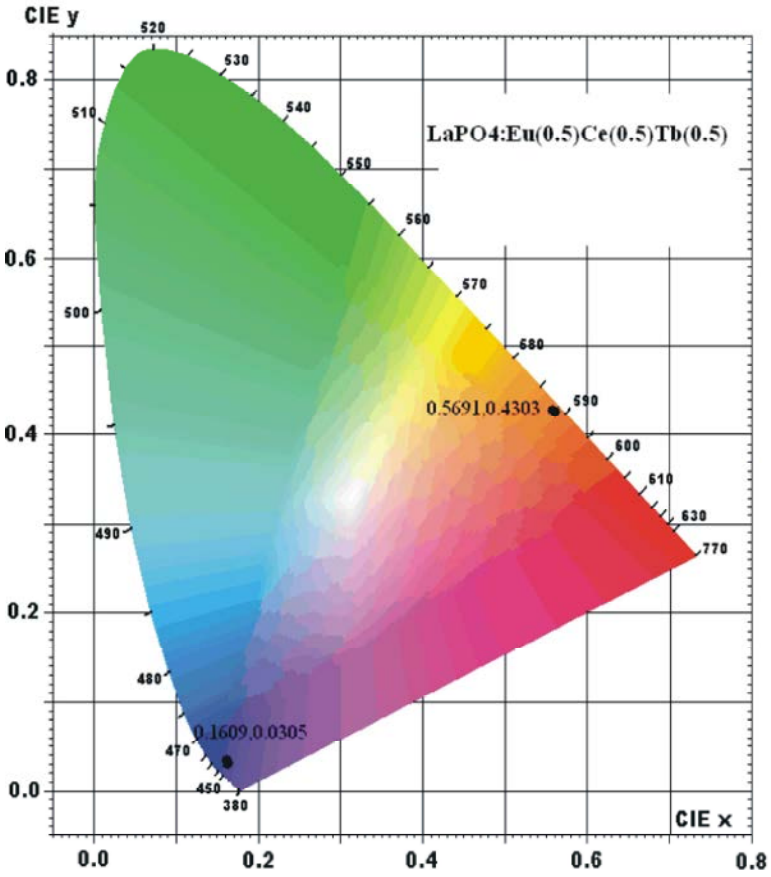

Fig. 6: CIE co-ordinates of pure $LaPO_4$ & $LaPO_4$:Eu, Ce, Tb

specimen particle size was measured by using laser based system Malvern Instrument, U.K. The mean particle size is 4.75µm.

Photoluminescence of $LaPO_4$ and $LaPO_4$: Eu (0.5)Ce(0.5)Tb(0.5) Phosphors: A series of $LaPO_4$:Eu^{3+}, Ce^{3+}, Tb^{3+} phosphors heated at 1200°C were prepared and the effect of Eu^{3+}, $Ce^{3+,}$ Tb^{3+} concentration on the emission intensity was investigated. Fig. 5(a) exhibits the PL excitation and emission spectra of pure $LaPO_4$ phosphor. In the excitation spectrum monitored under 400nm wavelength, the broadband ranging from 220-300nm with peaks at 254nm. The shape of the emission spectra and emission peak wavelength is independent of the excitation wavelengths. Upon excitation at 254nm wavelength, the emission spectrum of pure $LaPO_4$ phosphor emits a broad band range from 300-600nm with maximum intensity peak at 469(blue)nm as shown in Fig. 5a.

Fig. 5(b) exhibits the PL excitation and emission spectra of $LaPO_4$:$Eu^{3+}Ce^{3+}$ Tb^{3+}phosphor. In the excitation spectrum monitored under 612nm wavelength, the broad and intensive band ranging from 225-400nm with maximum peak at 269nm, related to a ligand-metal charge transfer between $PO^{3/4-}$ groups and Eu^{3+} ions [28]. The emission spectrum of $LaPO_4$:$Eu^{3+,}$ Ce^{4+} Tb^{3+}phosphor under 254nm excitation wavelength displays the characteristic red light with a number of narrow lines due to $^5D_0 \rightarrow {}^7F_{J=0,\ 1,\ 2,\ 3,\ 4}$ transitions of Eu^{3+}. The $^5D_0$-$^7F_0$ transition occurs as a unique, sharp and intense line, indicating the occupation of a site of low symmetry, in agreement with the monoclinic structure of this orthophosphate. The predominance of the hypersensitive, magnetic dipole transition $^5D_0$-$^7F_1$ (594nm) transition in the emission spectrum is determinant for the applicability of this material, a high emission orange colour purity is achieved. In the present case, the low contributions of the red (614nm) $^5D_0$-$^7F_2$ emission originate from the electric dipole transition and the high intensity of the $^5D_0$-$^7F_1$ (594nm) emission results in high color purities. The electric dipole transition is allowed when Eu^{3+} ion occupies a site without an inversion center and is sensitive to local symmetry. When Eu^{3+} ion occupies inversion center sites, the $^5D_0$-$^7F_1$ transition should be relatively strong, while the $^5D_0$-$^7F_2$ transition should be relatively weak [18]. Low intensity

peaks of Eu^{3+} ion were observed around 652 and 688nm assigned to the transitions of $^5D_0$- F_3 and D -$_0F_4$ $_r$especively. The typical emission peaks of terbium were observed around 488 and 545nm assigned to the transitions of $^5D_4$-^7F_J(J =6, 5) respectively and the emission of $^5D_4$-$^7F_3$ transition at 622 nm [29]. Ce^{3+} ions had a relatively broad absorption band from 200 to 300 nm with an allowed 4f–5d transition and transfered their energy to the doped Tb^{3+} ions emitting the green light. In this nanophosphor Ce^{3+} ions behave as sensitizer and Tb^{3+} ions act as luminescent center [30-33].

CIE Coordinates: The CIE co-ordinates of (chart -1931) were calculated by the Spectrophotometric method using the spectral energy distribution of pure $LaPO_4$ phosphor and $LaPO_4$:$Eu^{3+,}$ Ce^{3+}, Tb^{3+} phosphor as shown in Fig. 5. The color co-ordinates for pure $LaPO_4$ sample(A) are x = 0.16 and y = 0.03 and Eu, Ce, Tb doped $LaPO_4$ sample(B) sample are x = 0.57 and y = 0.43. From the Fig. 5, it was observed that the emission varies from blue to orange region. CIE 1931 chromaticity coordinates of prepared samples are acceptable for many optical applications [19, 20].

CONCLUSION

Pure $LaPO_4$ and $LaPO_4$:Eu^{3+}(0.5mol%) Ce^{3+}(0.5mol%) Tb^{3+} (0.5mol%) phosphor powders were successfully synthesized by the high temperature solid state reaction method and the luminescent properties of samples was studied.The XRD results reveal that the synthesized samples phosphors are well crystalline and assigned to the monoclinic crystal structure with a main (120) diffraction peak. No spurious diffractions due to crystallographic impurities are found. The width of diffraction peaks is broadened because of the small size of the crystallites. The grain sizes of the samples estimated from the SEM picture is larger than that obtained from XRD data. $LaPO_4$: Eu^3(0.5mol%) Ce^{3+}(0.5mol%) Tb^{3+} (0.5mol%) phosphor powders exhibit the characteristic emission Ce^{3+}lines and also exists energy transfer process between $LaPO_4$ and Eu^{3+}, Ce^{3+}, Tb^{3+} ions.

Under excitation, the intensity of transition from $^5D_0$-$^7F_1$ is higher than that from $^5D_0$-$^7F_2$. The Stoke shift and the FWHM of the emission were characteristic of a ligand-to-metal charge transfer(CT) emission. The photoluminescence results indicate that the $LaPO_4$: $Eu^{3+,}$ Ce^{3+}, Tb^{3+}phosphor have a strong orange $^5D_0$-$^7F_1$ transition. The typical emission peaks of terbium were observed around 488 and 545nm assigned to the transitions of $^5D_4$ -^7F_J(J =6, 5). The Commission International de 1'Eclairage [CIE] co-ordinates of pure $LaPO_4$ phosphor exhibit the excellent colour tunability of blue and Eu, Ce, Tb doped $LaPO_4$ phosphor reveals that the emission varies from blue to orange may make it to be a potential luminescent material.

ACKNOWLEDGEMENTS

The author, Niyaz Parvin Shaik, is gratefully thanking the University Grant Commission (UGC), New Delhi, India for financial assistance under Maulana Azad National Fellowship for Minority students.

REFERENCES

1. Xu, L., G. Guo, D. Uy, A. O'Neil, W.H. Weber, M.J. Rokosz and R.W. McCabe, 2004, J. Appl. Catal., B 50: 113
2. Yan, R.X., X.M. Sun, X. Wang, Q. Peng and Y.D. Li, 2005. Chem. Eur. J., 11: 2183.
3. Rajesh, K., P. Mukundan, P.K. Pillai, V.R. Nair and K.G.K. Warrier, 2004. Chem. Mater., 16: 2700.
4. Tang, C.C., Y. Bando, D. Golberg and R.Z. Ma, 2005. Angew. Chem. Int. Edn., 44: 576.
5. Lu, H.C., G.S. Yi, S.Y. Zhao, D.P. Chen, L.H. Guo and J. Cheng, 2004, J. Cheng, Mater. Chem., 14: 1336.
6. Adachi, G.Y. and N. Imanaka, 1998. Chem. Rev., 98: 1479.
7. Firsching, F.H. and S.N. Brune, 1991, J. Chem. Eng. Data., 36: 93.
8. Rouanel, A., J.J. Serra, K. Allaf and V.P. Orlovskii, 1981. Inorg. Mater, 17: 76.
9. Guo, Y., P. Woznicki, A. Barkatt, E.E. Saad and I.G. Talmy, 1996, J. Mater. Res., 11: 639.
10. Dexpert-Ghys, J., M.R. Mauricot, D. Faucher, 1996. J. Lumin., 69: 203.
11. Blasse, G. and B.C. Grabmaier, 1994., Luminescent Materials, Springer, Berlin.
12. Rao, R.P. and D.J. Devine, 2000. J. Lumin., pp: 87-89, 1260.
13. Pooping Yang, Zewei Quan, Chunxia Li, Zhiyao Hou, Wenxin Wang and Jun Lin, 2009. Journal of Solid State Chemistry, 182: 1045-1054.
14. Wang, L.Y. and Y.D. Li, 2006. Nano Letters, 6(8): 1645-1649.
15. Porcher, P., R. Saez and P.A. Caro, 1999, Rare Earths, Editorial Complutense, Madrid.

16., Bu¨nzli, J.C.G., 1989. In: J.C.G. Bu¨nzli, G.R. Choppin, (Eds.), Lanthanide Probes in Life, Chemical and Earth Sciences, Elsevier, Amsterdam.
17. Paulo C. De Sousa Filho and Osvaldo A. Serra, 2009. Journal of Luminescence, 129: 1664-1668.
18. Hashimoto, N., Y. Takada, K. Sato and S. Ibuki, 1991. J. Lumin., pp: 48-49, 893.
19. Miniscalco, W.J., 1991. J. Lightwave Technol., 9: 234.
0. Mullica, D.F., W.O. Milligan, D.A. Grossie, G.W. Beall amd L.A. Boatner, 1984. Inorg. Chim. Acta, 95: 231.
21. Dexpert-Ghys, J., R. Mauricot and M.D. Faucher, 1996. J. Lumin., 69: 203.
22. Rambabu, U., N.R. Munirathnam, T.L. Prakash and S. Buddhudu, 2002. Mater. Chem. Phys., 78: 160.
23. Kang, Y.C., E.J. Kim, D.Y. Lee and H.D. Park, 2002. J. Alloys. Compounds, 347(1-2): 266.
24. Meyssamy, H., K. Riwotzki, A. Kornowski, S. Naused and M. Haase, 1999. Adv. Mater., 11: 840.
25. Haase, M., K. Riwotzki, H. Meyssamy and A. Kornowski, 2000. J. Alloys Comp., 303-304, 191.
26. Color Calculator version 2, software from Radiant Imaging, Inc, (2007), http://radiant-imaging-color-calculator.software.informer.com/2.0/
27. Anderssona, J., S. Arevaa, B. Spliethoffb and M. Linde´na, 2005. Biomaterials, 26: 6827.
28. Fang, Y.P., A.W. Xu, R.Q. Song, H.X. Zhang, L.P. You, J.C. Yu and H.Q. Liu, 2003, J. Am. Chem. Soc., 125: 16025.
29. Martinus, H.V., 2005. Werts, Science Progress, 88(2): 101-131
30. Xin, J.I., Fei-Jian Zhu, Ha-Lei Zhai and Rui-Kang Tang, 2010. Front. Mater. Sci. China, 4(4): 382-386.
31. Kojima, Y., S. Doi, T. Yasue, 2002. Journal of the Ceramic Society of Japan, 110: 755-760.
32. Sohn, K.S., D.H. Park, S.H. Cho, B.I. Kim and S.I. Woo, 2006. Journal of Combinatorial Chemistry, 8(1): 44-49.
33. Ding, S., W. Zhang, B. Xu and J. Wang, Spectroscopy and Spectral Analysis, 21(3): 275-278.